ACS APPLIED MATERIALS & INTERFACES

Research Article

www.acsami.org

Synthesis of Palladium/Helical Carbon Nanofiber Hybrid Nanostructures and Their Application for Hydrogen Peroxide and Glucose Detection

Xueen Jia,[†] Guangzhi Hu,[†] Florian Nitze,[†] Hamid Reza Barzegar,[†] Tiva Sharifi,[†] Cheuk-Wai Tai,[‡] and Thomas Wågberg*[,†]

[†]Department of Physics, Umeå University, S-901 87 Umeå, Sweden

[‡]Department of Materials and Environmental Chemistry and Berzelii Center EXSELENT on Porous Materials, Arrhenius Laboratory, Stockholm University, Stockholm S-10691, Sweden

Supporting Information

ABSTRACT: We report on a novel sensing platform for H_2O_2 and glucose based on immobilization of palladium-helical carbon nanofiber (Pd-HCNF) hybrid nanostructures and glucose oxidase (GOx) with Nafion on a glassy carbon electrode (GCE). HCNFs were synthesized by a chemical vapor deposition process on a C_{60}-supported Pd catalyst. Pd-HCNF nanocomposites were prepared by a one-step reduction free method in dimethylformamide (DMF). The prepared materials were characterized by transmission electron microscopy (TEM), X-ray diffraction (XRD), scanning electron microscopy (SEM), and Raman spectroscopy. The Nafion/Pd-HCNF/GCE sensor exhibits excellent electrocatalytic sensitivity toward H_2O_2 (315 mA M^{-1} cm^{-2}) as probed by cyclic voltammetry (CV) and chronoamperometry. We show that Pd-HCNF-modified electrodes significantly reduce the overpotential and enhance the electron transfer rate. A linear range from 5.0 μM to 2.1 mM with a detection limit of 3.0 μM (based on the S/N = 3) and good reproducibility were obtained. Furthermore, a sensing platform for glucose was prepared by immobilizing the Pd-HCNFs and glucose oxidase (GOx) with Nafion on a glassy carbon electrode. The resulting biosensor exhibits a good response to glucose with a wide linear range (0.06−6.0 mM) with a detection limit of 0.03 mM and a sensitivity of 13 mA M^{-1} cm^{-2}. We show that small size and homogeneous distribution of the Pd nanoparticles in combination with good conductivity and large surface area of the HCNFs lead to a H_2O_2 and glucose sensing platform that performs in the top range of the herein reported sensor platforms.

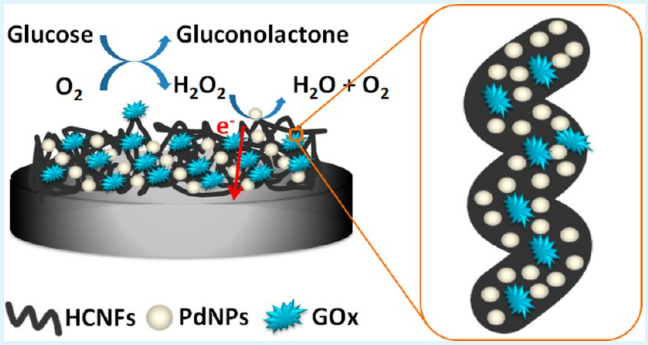

KEYWORDS: *hydrogen peroxide, glucose, helical carbon nanofibers, palladium, Nafion, nanoparticles, biosensors*

1. INTRODUCTION

Development of sensitive and stable glucose biosensors motivates researchers due to the high need for monitoring blood sugar, especially for patients suffering from diabetes.[1−3] Among the vast number of approaches explored in the past decades, glucose oxidase (GOx) represents one of the most frequently used enzymes due to its high sensitivity and unmatched selectivity.[4−10] Glucose detecting by such biosensors usually involves two steps. At first the immobilized GOx converts glucose and oxygen into gluconolactone and H_2O_2; second, H_2O_2 is oxidized to O_2 when a working potential is applied to the biosensor. An electric current proportional to glucose concentration is measured to quantify glucose. Hence H_2O_2 sensing plays an essential role in the determination of the blood glucose content but is also important in dyes, food, pharmaceutical industries, as well as environmental studies.[11−15]

Carbon nanomaterials such as carbon nanotubes, C_{60}, and graphene are suitable electrode modification materials and supports in biosensor applications due to their excellent charge transport capability, high mechanical strength, large surface area, high chemical stability, and good compatibility with biomaterials.[16−22] Palladium (Pd) is extensively used in catalytic applications because of many advantageous properties, including for example high catalytic efficiency and environmentally benign characteristics. Also, although palladium is rather expensive it is still considerably cheaper than platinum, the most frequently used catalyst in modern applications. Various different approaches have been pursued to incorporate Pd particles into various carbon supports for fabrication of Pd-modified electrodes for electrocatalysis.[23] Helical carbon

Received: September 5, 2013
Accepted: November 1, 2013
Published: November 1, 2013

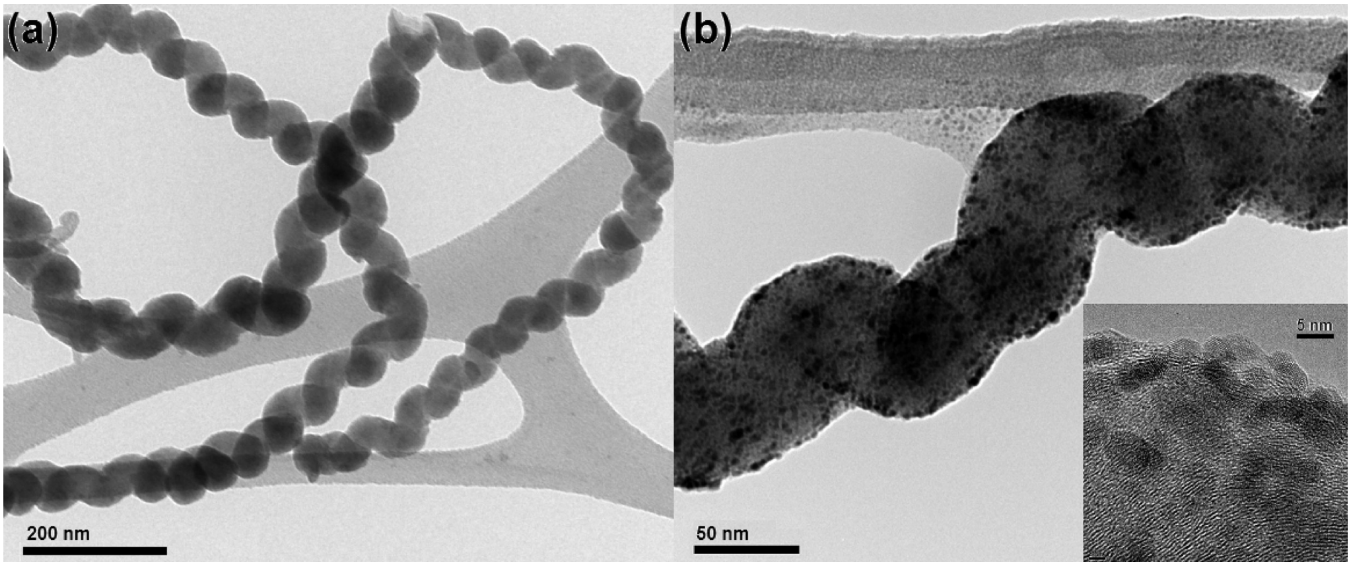

Figure 1. TEM images of (a) original HCNFs and (b) Pd nanoparticle decorated HCNFs (inset: HR-TEM of Pd-HCNFs).

nanofibers (HCNFs) are a less studied catalyst support although they possess equal or better properties than multiwalled carbon nanotubes.[24] In addition, HCNFs can be produced at relatively low temperatures and in large quantity, implying that they are a good candidate for high-performance catalysts in direct fuel cells.[25−27] The enhanced catalytic performance is generally attributed to an interaction between the metal nanocatalyst and the carbon support leading to modification of the electron density concurrent with a stabilization of crystalline surfaces. Also most carbon-based nanomaterials exhibit good conductivity and increased surface area which improves electrocatalytic performance.

Here, we report on the preparation of a novel biosensor platform based on Pd-HCNFs. The decoration of the HCNFs by palladium is achieved by a novel, highly efficient, yet environmentally benign method utilizing a one-step reduction free process in DMF. By modifying the glassy carbon electrode (GCE) by drop casting a dispersion of Pd-HCNFs we could prepare two sets of electrodes: one enzyme-free electrode comprising Nafion/Pd-HCNFs/GCE and one Nafion/GOx-Pd-HCNFs/GCE electrode. The composite materials have been investigated by TEM, Raman, and XRD, and our electrodes were characterized as a biosensor for H_2O_2 and glucose by means of CV and chronoamperometry. The H_2O_2 and glucose sensing properties were determined with an amperometric method at an applied potential of 0.5 V. We show that the Nafion/Pd-HCNFs/GCE and the Nafion/GOx-Pd-HCNFs/GCE sensors exhibit excellent sensing properties with detection limits of 3.0 μM and 0.03 mM for H_2O_2 and glucose, respectively. Due to the high homogeneity, good distribution, and small size of the anchored palladium nanoparticles concomitant with the excellent conductivity and high surface area of the HCNFs, our reported H_2O_2 and glucose sensing platforms exhibit sensing characteristics which rank among the very top level of the herein reported Pd-based biosensors. Concurrent with the good sensing properties of our glucose sensor platform, our method possesses several beneficial advantages: (i) The helical carbon nanofibers are produced by a palladium-catalyzed process, meaning that the final biosensor do not contain any of the common transition metals, such as cobalt or iron. This is different from most other carbon supports based on carbon nanotubes and carbon fibers and is compatible with in vivo studies due to the benign properties of the palladium. (ii) Our method for decorating the HCNFs is very simple and environmentally sound as it only involves a one-step reduction free process of the HCNF support in DMF. All other steps involve only direct mixtures of suspensions and drop-casting. This is a much more straightforward and fast process compared to those reported for biosensors with comparable properties.

2. EXPERIMENTAL SECTION

2.1. Chemicals. Nafion solution (5 wt % in water and light alcohols, DuPont, DE520) was purchased from Ion Power. *N*,*N*-Dimethylformamide (DMF), and Pd_2DBA_3 was purchased from Sigma Aldrich. H_2O_2 (VWR) was diluted to required concentrations before use. Glucose oxidase (from *Aspergillus niger*, type II, ≥15 000 unit/g, Sigma-Aldrich Co.) solution was also prepared before use by preparing a D-(+)-glucose (Sigma-Aldrich Co.) solution and leaving it overnight (12 h) to allow equilibration of anomers. As supporting electrolyte, 0.1 M phosphate buffer solution (PBS, pH 7.0) was employed. For aqueous solutions, distilled water was used. For all other reagents the quality was of analytical grade or better. Experiments were conducted at room temperature (~22 °C).

2.2. Preparation and Characterization of Pd-HCNFs. High-quality HCNFs were synthesized using Pd_2C_{60} as catalyst in a standard CVD system[27] followed by a one-step reduction and functionalization method of Pd nanoparticles in DMF solution. Briefly, 5 mg of Pd_2DBA_3 was mixed with 5 mL of DMF and then ultrasonicated for 3 min. An amount of 5 mg of HCNF was added into the above solution and stirred overnight for ca. 12 h at room temperature. A detailed description of the functionalization mechanism is reported elsewhere.[28] Thereafter, the suspension was filtered with a Millipore cellulose membrane (pore size: 0.22 μm) and washed with ethanol and water 3 times. The as-obtained Pd-HCNFs were dried at 60 °C in a vacuum oven overnight.

Structural analysis was carried out by transmission electron microscopy (JEOL JEM-2100F) with an acceleration voltage of 200 kV on samples that were dispersed on holey carbon film-coated copper grids. Raman spectroscopy was conducted on a Renishaw InVia Raman spectrometer with a CCD detector using an excitation wavelength of 785 nm. X-ray diffraction of Pd-HCNFs was performed on a Siemen's D5000 using Cu Kα (λ = 1.5406 Å) radiation.

2.3. Electrode Modification and Electrocatalytic Measurement. The electrochemical experiments were performed on an

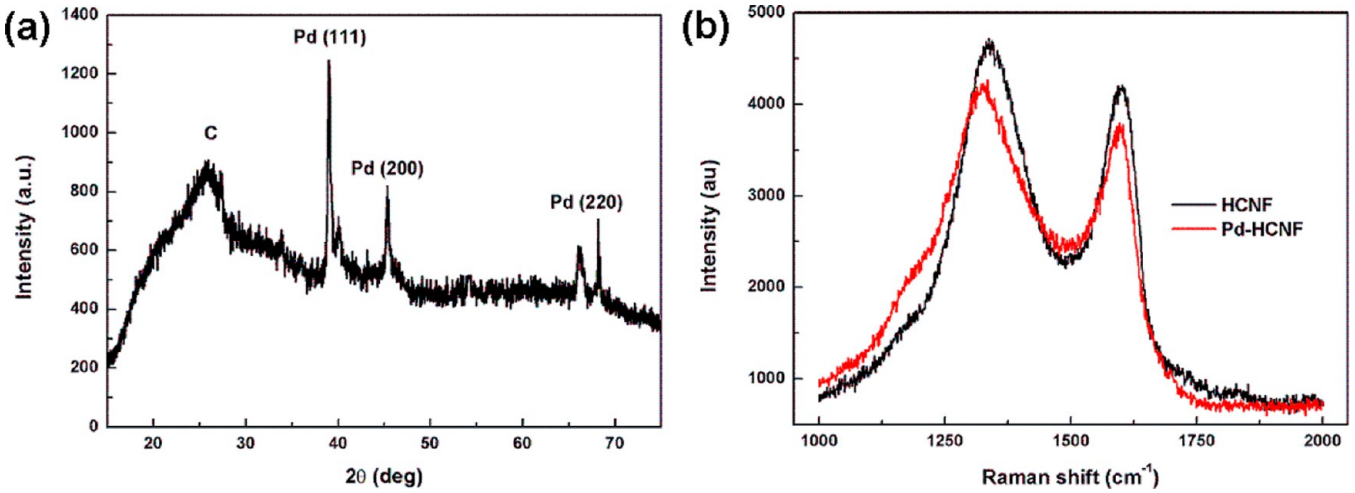

Figure 2. (a) XRD patterns of Pd-HCNF nanostructures. (b) Raman spectra of Pd-HCNF nanostructures (red curve) and HCNFs (black curve).

Autolab PGSTAT30 with a three-electrode cell at room temperature. A Pt wire and a Ag/AgCl electrode were used as counter and reference electrodes, respectively. A GCE (d = 3 mm) was used as a working electrode.

The GCE surface was highly polished with alumina paste, washed by distilled water, and finally rinsed with ethanol. Then the GCE surface was coated with 5.0 μL of a 1 mg/mL Pd-HCNF suspension. After drying at room temperature, 5.0 μL of a 0.5% Nafion solution was further drop casted onto the electrode surface (electrode area = 0.07 cm^{-2}). For enzyme electrode preparation, 5.0 μL of a 2 mg GO_x in 1 mL of Pd-HCNF mixed suspension was coated on the GCE surface and dried in a fridge (4 °C) followed by drop casting 5.0 μL of a 0.5% Nafion solution onto the electrode surface. The Nafion/Pd-HCNFs/GCE and Nafion/GOx/Pd-HCNFs/GCE electrodes were washed with distilled water before and after each experiment.

3. RESULTS AND DISCUSSION

3.1. Characterization of Pd-HCNFs. Figure 1a shows a TEM image of HCNFs with 40−60 nm in diameter. After coincubation with Pd_2DBA_3 in DMF, numerous individual dark nanoparticles appear on the surface of the gray HCNFs. TEM images (Figure 1b) show that nanosized particles are highly dispersed and well anchored on the HCNFs. The average particle size is about 5 nm. The high-resolution TEM (HRTEM) image (inset in Figure 1b) shows lattice fringes of both graphitic sheets of HCNFs and Pd nanoparticles. More TEM images are presented in the Supporting Information (Figure S1).

The crystalline structure of the Pd nanoparticles is further manifested by the X-ray diffraction pattern shown in Figure 2a. The peak located at 25° in the XRD patterns is assigned to (0 0 2) in the hexagonal structure of the HCNFs. The three strong peaks at 2θ = 40°, 48°, and 70° are assigned to the (1 1 1), (2 0 0), and (2 2 0) reflections of face-centered cubic (fcc) Pd. It is known that these sharp peaks represent the approximately 40 nm large interior Pd particles that originate from the synthesis of the HCNFs.[24,26] The externally decorated Pd particles are instead represented by the smaller, broader, and upshifted side peaks. Most clear is the upshifted peak around 2θ = 40°. The wider full width half-maximum (fwhm) and the upshift are rationalized by a smaller crystallite size[29] (around 5 nm) as well as a slight decrease in lattice parameter compared to bulk palladium.

Figure 2b shows the Raman spectra of HCNFs and Pd-HCNFs. Both spectra contain the characteristic D band at ~1330 cm^{-1} and G band at 1570 cm^{-1}. The D band is generally associated with defects located along the nanofiber side-walls, while the G band is attributed to tangential vibration modes typical for sp^2 carbon materials such as graphite and carbon nanotubes.[30] The larger value of I_D/I_G (1.45) for Pd-HCNFs compared to I_D/I_G = 1.38 for the pristine HCNFs signals a decrease in crystallinity following the functionalization of the Pd-HCNFs which is further manifested by the wider fwhm of the Pd-HCNF D-band as well as a significant increase of a shoulder peak at 1200 cm^{-1}. All these observations are in line with a large number of sidewall defects in the functionalized Pd-HCNFs.

3.2. Electrochemical Behavior of the Modified Electrode. The voltammetric response of H_2O_2 on the modified electrode was recorded by CV. In Figure 3a typical CV of 0.5 mM H_2O_2 in 0.1 M PBS at pH 7.0 is shown, recorded at the Nafion/GCE and the Nafion/Pd-HCNFs/GCE electrode.

For pure GCE, there is no difference with or without H_2O_2. When the GCE was modified only by HCNFs, besides the enhancement of the background current, we do not find any peak and current response (not shown). After modification of

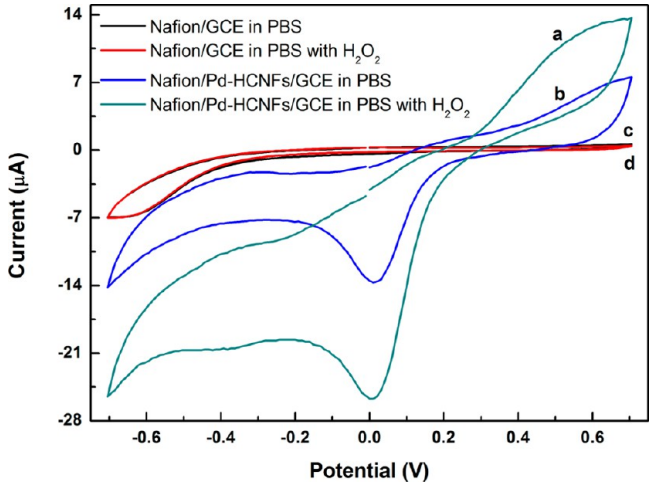

Figure 3. Cyclic voltammograms of the Nafion/Pd-HCNFs/GCE (a, b) and Nafion/GCE (c, d) with and without 0.5 mM H_2O_2 in 0.1 M PBS (pH 7.0). Scan rate: 50 mV/s.

dx.doi.org/10.1021/am4037383 | ACS Appl. Mater. Interfaces 2013, 5, 12017−12022

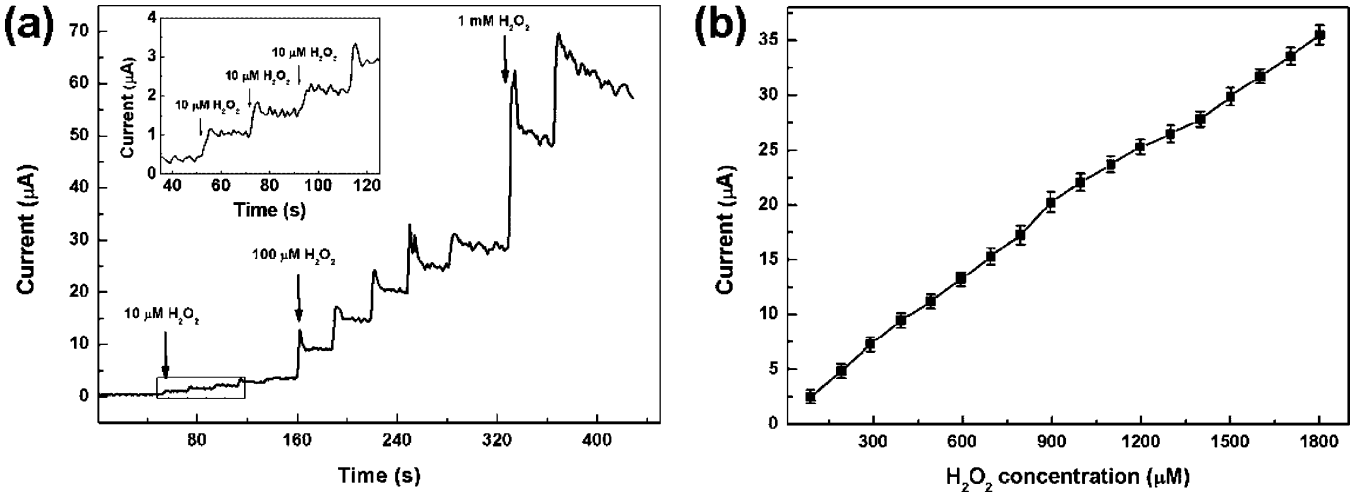

Figure 4. (a) Amperometric response of the Nafion/Pd-HCNFs/GCE when successively adding different amounts of H_2O_2 into 10 mL stirring PBS (pH 7.0) at the potential of 0.5 V (inset indicated by arrows with marked concentrations). (b) The corresponding calibration curve.

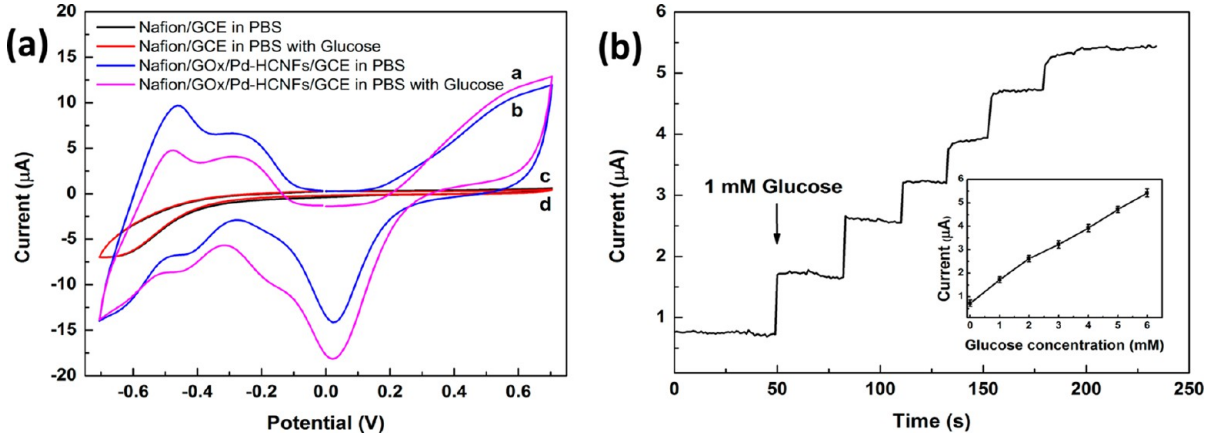

Figure 5. (A) Cyclic voltammograms of Nafion/GOx/Pd-HCNFs/GCE (a, b) and Nafion/GCE (c, d) with and without 1 mM glucose in 0.1 M PBS (pH 7.0). Scan rate: 50 mV/s. (B) Amperometric response of the Nafion/GOx/Pd-HCNFs/GCE when successively adding 10 μL of 1 M glucose into 10 mL of stirring PBS (pH 7.0) at the potential of 0.5 V. Inset: The corresponding calibration curve.

Pd-HCNFs, the catalytic current keeps increasing significantly during the anodic scan, and a sharp peak is observed around 0.05 V with a sufficiently high current response during the cathodic scan. Through these observations it is clear that the Pd nanoparticles exhibit an enhanced electrocatalytic efficiency by their adhesion on the HCNFs. This is rationalized by a high ability of the Pd-HCNFs to transfer the electrons involved in the catalytic reaction and hence sensitively trace the presence of H_2O_2 electrochemically. Figure S3 (Supporting Information) shows the cyclic voltammograms of Nafion/Pd-HCNFs/GCE at various scan rates. The anodic and cathodic peak currents increase linearly with scan rate from 10 to 125 mV s^{-1}, signaling that the electrochemical reaction in the Pd-HCNF−composite film is a surface-confined reversible process.

3.3. Electrocatalytic Detection of H_2O_2. The detection of H_2O_2 for the Nafion/Pd-HCNFs/GCE was evaluated by an amperometric technique. In this work, the applied potentials of 0.5 and 0.05 V (as shown in Figure S4, Supporting Information) were chosen.

Figure 4a illustrates the chronoamperometric response of the modified electrode by subsequently adding 10 mL of H_2O_2 in PBS at an applied potential of 0.5 V. The inset of Figure 4a presents the current response at low concentrations of H_2O_2. The calibration curve of the response currents versus H_2O_2 concentration in Figure 4b shows good linearity all the way down to 5.0 μM H_2O_2 concentration. The current density of the H_2O_2 reduction obtained at the Nafion/Pd-HCNFs/GCE is high, rendering a very good sensitivity (change of current density per unit concentration of H_2O_2) of about 315 mA M^{-1} cm^{-2}. The electrode response is reasonably fast, and we observe a steady-state signal within 10 s. The linear regression equation is: I (μA) = 0.1892C (mM) + 1.72488, with a 0.9949 correlation coefficient. To determine the detection limit, cronoamperometry was applied by sampling from 5.0 to 1900 μM (Figure 4b). On the basis of the signal-to-noise ratio (S/N = 3) a detection limit as low as 3.0 μM was estimated.

3.4. Glucose Biosensor Based on Pd-HCNFs. To fabricate a glucose biosensor, GOx was immobilized on a Pd-HCNFs/GCE. The morphology of the fabricated sensor was characterized by SEM as shown in Figure S2 (Supporting Information). The modified electrode is porous but yet uniformly deposited on the substrate.

Figure 5(A) reveals the voltammetric responses of the fabricated Nafion/GOx/Pd-HCNFs/GCE. Similar to the H_2O_2 case shown in Figure 3, it is obvious that for pure a GCE there is no difference before and after adding glucose. For the

Table 1. Performance for Different Types of Glucose Sensing Platforms and the Protocol for Preparation[a]

sensor platform	protocol	sensitivity ($mA\ cm^{-2}\ M^{-1}$)	response time (s)	linear range (mM)	detection limit (μM)	ref
Nafion/GOx/Pd-HCNFs/GCE	reduction-free self-assembly	13	<5	0.06−6	30	this work
GO_x/Pd/CS-GR/GCE	self-assembly	31	<5	0.001−1	0.2	31
Nafion/CS-GA-GO_x/-Pd/Pt-MWNTs/GCE	electrodeposition	110	<5	0.06−14	30	32
Nafion/GOx/Pd-MWNTs/GCE	electrodeposition	40	<10	0.2−12	150	33
Nafion/GO_x/Pd-PEDOT/GCE	electrodeposition	1.6		0.5−30	75	34
GO_x/Pt-PPy/Anodisc	template growth	7.4	<4	0.5−10.4	30	35
Nafion/GA-GOx/MWCNTs-Pd/GCE	cross-linking/ self-assembly	38	<10	0.01−10	0.4	36
GOx/CS/CNT/Au	electrodeposition	6.7	<3	0.005−8	2	37
GOx/CS/Au-GR/Au	reduction self-assembly	17		2−10	180	38

[a]Abbrevations: CS, Chitosan; GA, glutaraldehyde; GR, Graphene; PEDOT, poly(3,4-ethylendioxythiophene)-nanofibers; Anodisc, porous aluminum oxide; PPy, polypyrrole.

Nafion/GOx/Pd-HCNFs/GCE electrode, after adding 1 mM glucose, the catalytic current keeps increasing during the anodic scan and cathodic scan. It can be deduced that the presence of H_2O_2 transferred from glucose under the catalyzation of GOx. Figure 5(B) depicts chronoamperometric responses of the fabricated Nafion/GOx/Pd-HCNFs/GCE for successive addition of 1.0 mM glucose in 0.1 M PBS at potential 0.5 V. The response increases stepwise with increasing concentrations of glucose providing a linear current response for glucose in the concentration range of 1.0−6.0 mM with a correlation coefficient of 0.994 (the linear regression equation is I (μA) = 0.8986C (mM) + 0.7643), giving a sensitivity of 13 mA M^{-1} cm^{-2}. The limit of detection (LOD) is calculated to be 30.0 μM. The linear range is well adapted to the concentration of glucose in human blood, which ranges between 4 and 6 mM. Compared to single noble metal enzymatic GO_x-based amperometric sensors fabricated on other nanostructures the proposed biosensor presents a wider linear range and yet a satisfactory LOD which is ascribed to the preeminent sensitivity of the Nafion/Pd-HCNFs/GCE for H_2O_2. We note also that the method to prepare our sensor platform is significantly easier and faster than most other approaches reported earlier.

In Table 1, we give a comparison of our developed sensor with enzymatic sensors based on single noble metal nanoparticles supported on various carbon nanostructures. We have included also one report of bimetallic nanoparticles to indicate that bimetallic noble metals usually achieve higher sensitivity, however, with a cost of more demanding preparation procedures.

3.5. Interference Study. An important characteristic for glucose biosensors is so-called interference studies which probe the sensor-selective response for glucose in the presence of other interfering species. Such an anti-interference ability by the chronoamperometric method is shown in Figure 6 using 0.1 mM ascorbic acid (AA) and 0.1 mM uric acid (UA), which are the common interfering electroactive substances for a H_2O_2 biosensor.

The two selected acids caused an increase of only 1.6% and 7.0% in the oxidation current of 1.0 mM glucose at 0.5 V, respectively. This is explained by the ability of Nafion to reduce the permeability of negatively charged substances.[33,39] Furthermore, Figure S6 (Supporting Information) shows the amperometric response for the biosensor after subsequent injection of 0.1 mM H_2O_2, 1.0 mM H_2O_2, 1.0 mM glucose, 0.1 mM AA, 0.1 mM UA, and 1.0 mM H_2O_2 at 0.05 V. These particular concentrations were used because the level of the endogenous AA and UA is about 0.125 and 0.33 mM in blood, respectively.[40,41] No significant current response of AA, glucose, and UA was observed compared to those of H_2O_2, manifesting high selectivity of the proposed biosensor.

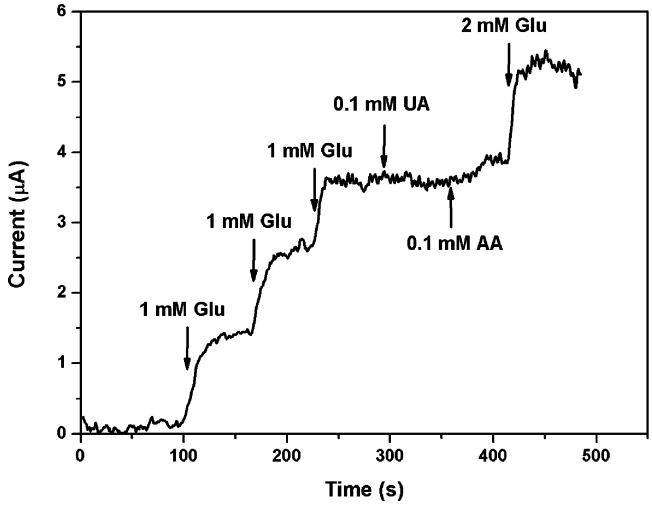

Figure 6. Amperometric response of the glucose biosensor upon addition of 1.0 mM glucose for triple, 0.1 mM uric acid (UA), 0.1 mM ascorbic acid (AA), and 2.0 mM glucose. The applied potential is 0.5 V.

3.6. Reproducibility and Stability. It is essential for a biosensor to test the reproducibility and long-term stability. The reproducibility of our Pd-HCNF sensor was tested by measuring the response to 5 mM glucose for five different enzyme electrodes prepared under the same conditions. The results reveal a spread in the performance (R.S.D.) of 4.8% as shown in Figure S6 (Supporting Information), signaling a satisfactory reproducibility. To further explore the long-term stability, measurements were made with one week intervals (when not in use, the biosensor was stored in a dry condition at 4 °C). Also these tests showed desirable properties revealing that the biosensor retained 93% of its original current response after one week and approximately 84% after one month.

4. CONCLUSIONS

We demonstrate a facile preparation of a H_2O_2 and glucose biosensor by using a Pd-HCNFs support. The synthesized Pd-HCNFs provide enhanced electrocatalytic performance for H_2O_2 reduction in neutral media. The as-prepared Nafion/Pd-

HCNF/GCE exhibits a high sensitivity, a wide linear detection range, and very good selectivity for H_2O_2 detection. The fabricated Nafion/GOx/Pd-HCNFs/GCE biosensor shows very good attributes for glucose sensing. Compared to single noble metal enzymatic GO_x-based amperometric sensors fabricated on other nanostructures the reported biosensor exhibits a wider linear range and yet a satisfactory detection sensitivity. This is ascribed to the preeminent sensitivity of Nafion/Pd-HCNFs/GCE for H_2O_2. The sensor shows a very good long-term stability and high reproducibility and high reproducibility, explained by the excellent properties of HCNFs, such as high number of anchoring sites for the Pd nanoparticles and good conductivity. We also note that the method to prepare our sensor platform is significantly easier and faster than most other approaches reported earlier.

■ ASSOCIATED CONTENT

Ⓢ Supporting Information

Additional SEM images of the Nafion/GOx/Pd-HCNFs/GCE biosensor and electrochemical characterization. This material is available free of charge via the Internet at http://pubs.acs.org.

■ AUTHOR INFORMATION

Corresponding Author

*E-mail: thomas.wagberg@physics.umu.se.

Notes

The authors declare no competing financial interest.

■ ACKNOWLEDGMENTS

This work has been supported by Vetenskapsrådet (dnr-2010 3973), Ångpanneföreningen, Gustaf Richerts stiftelse. T. Wågberg thanks Kempestiftelsen for generous support. T. Wågberg and G. Z. Hu thank Wenner-Gren stiftelsen for support. T. Sharifi thanks Kempestiftelsen for generous support. F. Nitze thanks Gustaf Richerts stiftelse. We acknowledge the vibrational spectroscopy platform at Umeå University (VISP). The Knut and Alice Wallenberg Foundation is acknowledged for an equipment grant for the electron microscopy facilities in Stockholm University.

■ REFERENCES

(1) Heller, A.; Feldman, B. *Chem. Rev.* **2008**, *108*, 2482−2505.
(2) Wang, J. *Chem. Rev.* **2007**, *108*, 814−825.
(3) Chen, A.; Holt-Hindle, P. *Chem. Rev.* **2010**, *110*, 3767−3804.
(4) Clark, L. C.; Lyons, C. *Ann. N.Y. Acad. Sci.* **1962**, *102*, 29−45.
(5) Shi, L.; Lu, Y.; Sun, J.; Zhang, J.; Sun, C.; Liu, J.; Shen, J. *Biomacromolecules* **2003**, *4*, 1161−1167.
(6) Crouch, E.; Cowell, D. C.; Hoskins, S.; Pittson, R. W.; Hart, J. P. *Anal. Biochem.* **2005**, *347*, 17−23.
(7) Cosnier, S.; Mousty, C.; Cui, X.; Yang, X.; Dong, S. *Anal. Chem.* **2006**, *78*, 4985−4989.
(8) Fu, Y.; Chen, C.; Xie, Q.; Xu, X.; Zou, C.; Zhou, Q.; Tan, L.; Tang, H.; Zhang, Y.; Yao, S. *Anal. Chem.* **2008**, *80*, 5829−5838.
(9) Sakslund, H.; Wang, J.; Hammerich, O. *J. Electroanal. Chem.* **1994**, *374*, 71−79.
(10) Niu, X. H.; Chen, C.; Zhao, H. L.; Chai, Y.; Lan, M. B. *Biosens. Bioelectron.* **2012**, *36*, 262−266.
(11) Liu, S.; Ju, H. *Biosens. Bioelectron.* **2003**, *19*, 177−183.
(12) Lu, X.; Zhou, J.; Lu, W.; Liu, Q.; Li, J. *Biosens. Bioelectron.* **2008**, *23*, 1236−1243.
(13) Shu, X.; Chen, Y.; Yuan, H.; Gao, S.; Xiao, D. *Anal. Chem.* **2007**, *79*, 3695−3702.
(14) Cui, Z. M.; Li, N. W.; Zhou, X. C.; Liu, C. P.; Liao, J. H.; Zhang, S. B.; Xing, W. *J. Power Sources* **2007**, *173*, 162−165.
(15) Luo, X.-L.; Xu, J.-J.; Zhao, W.; Chen, H.-Y. *Biosens. Bioelectron.* **2004**, *19*, 1295−1300.
(16) Zhu, Z. G.; Garcia-Gancedo, L.; Flewitt, A. J.; Xie, H. Q.; Moussy, F.; Milne, W. I. *Sensors* **2012**, *12*, 5996−6022.
(17) Guldi, D. M.; Rahman, G. M. A.; Zerbetto, F.; Prato, M. *Acc. Chem. Res.* **2005**, *38*, 871−878.
(18) Daniel, S.; Rao, T. P.; Rao, K. S.; Rani, S. U.; Naidu, G. R. K.; Lee, H.-Y.; Kawai, T. *Sens. Actuators, B* **2007**, *122*, 672−682.
(19) Lin, Y.; Taylor, S.; Li, H.; Fernando, K. A. S.; Qu, L.; Wang, W.; Gu, L.; Zhou, B.; Sun, Y.-P. *J. Mater. Chem.* **2004**, *14*, 527−541.
(20) Willner, I.; Willner, B. *Nano Lett.* **2010**, *10*, 3805−3815.
(21) Yang, J.; Deng, S.; Lei, J.; Ju, H.; Gunasekaran, S. *Biosens. Bioelectron.* **2011**, *29*, 159−166.
(22) You, J. M.; Jeong, Y. N.; Ahmed, M. S.; Kim, S. K.; Choi, H. C.; Jeon, S. *Biosens. Bioelectron.* **2011**, *26*, 2287−2291.
(23) Willner, I.; Willner, B.; Katz, E. *Bioelectrochemistry* **2007**, *70*, 2−11.
(24) Nitze, F.; Mazurkiewicz, M.; Malolepszy, A.; Mikolajczuk, A.; Kedzierzawski, P.; Tai, C. W.; Hu, G. Z.; Kurzydlowski, J. K.; Stobinski, L.; Borodzinski, A.; Wågberg, T. *Electrochim. Acta* **2012**, *63*, 323−328.
(25) Hu, G. Z.; Nitze, F.; Sharifi, T.; Barzegar, H. R.; Wågberg, T. *J. Mater. Chem.* **2012**, *22*, 8541−8546.
(26) Hu, G. Z.; Nitze, F.; Barzegar, H. R.; Sharifi, T.; Mikolajczuk, A.; Tai, C. W.; Borodzinski, A.; Wågberg, T. *J. Power Sources* **2012**, *209*, 236−242.
(27) Nitze, F.; Abou-Hamad, E.; Wågberg, T. *Carbon* **2011**, *49*, 1101−1107.
(28) Hu, G. Z.; Nitze, F.; Xueen, J.; Sharifi, T.; Barzegar, H. R.; Wågberg, T. *RSC Adv.* **2013**, DOI: 10.1039/C3RA42652A.
(29) Patterson, A. L. *Phys. Rev.* **1939**, *56*, 978−982.
(30) Sharifi, T.; Nitze, F.; Berzaghui, H. R.; Tai, C. W.; Mazurkiewicz, M.; Malopeszy, A.; Stobinski, L.; Wågberg, T. *Carbon* **2012**, *50*, 3535−3541.
(31) Zeng, Q.; Cheng, J. S.; Liu, X. F.; Bai, H. T.; Jiang, J. H. *Biosens. Bioelectron.* **2011**, *26*, 3456−3463.
(32) Chen, K. J.; Lee, C. F.; Rick, J.; Wang, S. H.; Liu, C. C.; Hwang, B. J. *Biosens. Bioelectron.* **2012**, *33*, 75−81.
(33) Lim, S. H.; Wei, J.; Lin, J. Y.; Li, Q. T.; KuaYou, J. *Biosens. Bioelectron.* **2005**, *20*, 2341−2346.
(34) Santhosh, P.; Manesh, K. M.; Uthayakumar, S.; Komathi, S.; Gopalan, A. I.; Lee, K. P. *Bioelectrochemistry* **2009**, *75*, 61−66.
(35) Ekanayake, E.; Preethichandra, D. M. G.; Kaneto, K. *Biosens. Bioelectron.* **2007**, *23*, 107−113.
(36) You, J. M.; Jeon, S. *Electroanalysis* **2011**, *23*, 2103−2108.
(37) Zhou, Q. M.; Xie, Q. J.; Fu, Y. C.; Su, Z. H.; Jia, X.; Yao, S. Z. *J. Phys. Chem. B* **2007**, *111*, 11276−11284.
(38) Shan, C. S.; Yang, H. F.; Han, D. X.; Zhang, Q. X.; Ivaska, A.; Niu, L. *Biosens. Bioelectron.* **2010**, *25*, 1070−1074.
(39) Shankaran, D. S.; Uehara, N.; Kato, T. *Anal. Chim. Acta* **2003**, *478*, 321−327.
(40) Wang, J.; Thomas, D. F.; Chen, A. *Anal. Chem.* **2008**, *80*, 997−1004.
(41) Meng, L.; Jin, J.; Yang, G.; Lu, T.; Zhang, H.; Cai, C. *Anal. Chem.* **2009**, *81*, 7271−7280.